Impact of Delays on a Consensus-based Primary Frequency Control Scheme for AC Systems Connected by a Multi-Terminal HVDC Grid

Jing Dai, Yannick Phulpin
Supélec, France
{jing.dai, yannick.phulpin}@supelec.fr

Alain Sarlette, Damien Ernst
University of Liège, Belgium
{alain.sarlette, dernst}@ulg.ac.be

Abstract

This paper addresses the problem of sharing primary frequency control reserves among non-synchronous AC systems connected by a multi-terminal HVDC grid. We focus on a control scheme that modifies the power injections from the different areas into the DC grid based on remote measurements of the other areas' frequencies. This scheme is proposed and applied to a simplified system in a previous work by the authors. The current paper investigates the effects of delays on the control scheme's effectiveness. The study shows that there generally exists a maximum acceptable delay, beyond which the areas' frequency deviations fail to converge to an equilibrium point. This constraint should be taken into account when commissioning such a control scheme.

1. Introduction

Frequency stability is one of the major concerns for power system operators [1]. It deals with the power system's ability to return to its nominal frequency after a severe disturbance resulting in a power imbalance. To maintain frequency stability, system operators have developed frequency control schemes, which are usually classified according to the time scale of their actions [2]. The actions corresponding to the shortest time scale are usually referred to as "primary frequency control". It consists of local automatic adjustment, within a few seconds after the disturbance, of the generators' power output based on locally measured frequency variations. The power margins that a generator provides around its scheduled output are named "primary reserves".

In a synchronous AC system, as the average frequency in the time frame of several seconds can be considered identical everywhere, the efforts of the generators participating in primary frequency control sum up within the area. Therefore, larger systems usually experience lower frequency deviations and have lower costs – per MWh – associated to primary frequency control reserves. This has been a significant motivation for interconnecting regional and national systems to create large-scale power systems, such as the UCTE network.

The development of high voltage direct current (HVDC) systems for bulk power transmission over long distances [3] and underground cable crossings opens new perspectives for interconnecting non-synchronous areas. In this context, it is generally expected that the power flows through an HVDC system are set at scheduled values, while frequencies of the AC areas remain independent. In a previous paper [4], we discuss the possibility of using the fast power-tracking capability of HVDC converters to share primary reserves among non-synchronous areas connected by a DC grid. In the same paper, a control scheme for the HVDC converters is also proposed. It is based on the body of work on consensus problems and relates the problem of sharing primary reserves between the different AC areas to the problem of making the frequency deviations in these areas converge rapidly to the same value.

Both the theoretical study and the simulation results reported in [4] show that, under some restrictive assumptions, the scheme can allow a reduction of the requirements in terms of the primary reserves in every AC area. One of these assumptions is that the information on the frequency of one area is instantaneously available to another area of the HVDC system. However, in practice, both measurement and communication introduce delays, which can reach up to a few seconds [5]. As this may challenge the effectiveness of the control strategy, this paper aims to extend the previous findings to more realistic cases by considering the effects of those delays. The analytical part of our study proves a unique equilibrium point for the

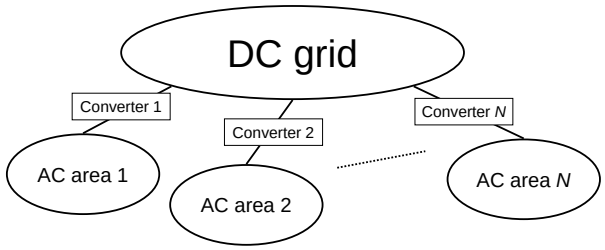

Figure 1. A multi-terminal HVDC system connecting N AC areas via converters.

system following a step change in the load of one AC area. In addition, we provide, under some restrictive assumptions on the power system, conditions under which this equilibrium point is reached. We also report simulation results showing, among others, that delays can indeed cause stability problems.

The paper is organized as follows. Section 2 describes a multi-terminal HVDC system model. Section 3 recalls the control scheme proposed in [4] and adds delays to it. Section 4 analyzes stability of a system with such dynamics. Section 5 presents a benchmark system and simulation results.

2. Multi-terminal HVDC system model

We consider a system with N AC areas, as shown in Fig. 1. The system has three types of components: a DC grid, N non-synchronous AC areas, and N converters that interface the AC areas with the DC grid.

The model aims to reproduce the main characteristics of the frequency of every AC area over a period of several tens of seconds. For notational convenience, the time dependency of the variables is not explicitly mentioned in the equations (i.e., we write x instead of $x(t)$) where it is not necessary.

2.1. AC area

The model of each AC area consists of two components, an aggregated generator and a load, both connected to the AC side of the HVDC converter.

The mechanical dynamics of the generator for area $i, \forall i \in \{1, \dots, N\}$ is described by the equation of motion

$$2\pi J_i \frac{df_i}{dt} = \frac{P_{mi} - P_{ei}}{2\pi f_i} - 2\pi D_{gi}(f_i - f_{nom,i}) \quad (1)$$

where f_i is AC area i's frequency, and $f_{nom,i}$ its nominal value; P_{mi} and P_{ei} are the mechanical power input and the electrical power output of the generator of area i, respectively; and J_i and D_{gi} are the moment of inertia and the damping factor of this generator. The power balance within this area requires

$$P_{ei} = P_{li} + P_i^{dc} \quad (2)$$

where P_{li} is the load demand of area i and P_i^{dc} is the power injection from this area into the DC grid.

The AC area's frequency is regulated by the speed governor of the generator, which observes the rotating speed of the shaft and adjusts P_{mi} accordingly, following

$$T_{smi} \frac{dP_{mi}}{dt} = P_{mi}^o - P_{mi} - \frac{P_{mi}^{\max}}{\sigma_i} \frac{f_i - f_{nom,i}}{f_{nom,i}} \quad (3)$$

where σ_i is the generator droop, T_{smi} the time constant of the servomotor, $P_{mi}^{\max}$ the maximum mechanical power available from the turbine, and P_{mi}^o the reference value for P_{mi} when $f_i = f_{nom,i}$. In practice, P_{mi}^o is refreshed by the secondary frequency controller at a relatively low pace. For instance, its time constant is a few minutes in the UCTE network [5]. Consequently, we assume in this paper that P_{mi}^o remains constant.

A static load model is used to represent the load

$$P_{li} = P_{li}^o \cdot (1 + D_{li}(f_i - f_{nom,i})) \quad (4)$$

where P_{li}^o is the power demand at $f_{nom,i}$ and D_{li} the frequency sensitivity factor.

2.2. DC network

As the electrical time constant of a DC grid is of the order of several milliseconds [6], transient dynamics of the DC grid is not considered in our model.

To take into account the general case where there exist nodes that are not connected to any AC area, we suppose that there are in total $M \geq N$ nodes in the DC grid and that node i is connected to AC area i via converter i, $\forall i \in \{1, \dots, N\}$. Then, the power transferred from node i to node j within the DC network, denoted by P_{ij}^{dc}, can be expressed as:

$$P_{ij}^{dc} = \frac{V_i^{dc}(V_i^{dc} - V_j^{dc})}{R_{ij}^{dc}} \quad (5)$$

where V_i^{dc} and V_j^{dc} are the voltages at nodes i and j, respectively, and R_{ij}^{dc} is the resistance between these two nodes. If nodes i and j are not directly connected, R_{ij}^{dc} is considered equal to infinity. Note that there must be either a direct or an indirect connection between any two nodes, otherwise the DC grid would be made of several parts which are not connected to each other.

The power balance at node i satisfies

$$\sum_{j=1}^{M} P_{ij}^{dc} = \begin{cases} P_i^{dc} & \text{for } i \leq N \ , \\ 0 & \text{for } i > N \ . \end{cases} \quad (6)$$

Replacing P_{ij}^{dc} by (5), we can write (6) in matrix form as the nonlinear relation

$$\mathbf{P}^{dc} = diag(V_1^{dc}, \ldots, V_M^{dc})\, A\, \mathbf{V}^{dc} \quad (7)$$

where

- $\mathbf{P}^{dc}$ is a vector of length M with the first N components equal to $P_1^{dc}, \ldots, P_N^{dc}$ and the last $M - N$ components equal to 0.
- $\mathbf{V^{dc}}$ is a vector containing the DC voltages $V_1^{dc}, \ldots, V_M^{dc}$.
- the components of matrix A are defined as

$$[A]_{ij} = \begin{cases} -\dfrac{1}{R_{ij}} & \text{for } i \neq j \ , \\ \sum_j \dfrac{1}{R_{ij}} & \text{for } i = j \ . \end{cases}$$

2.3. HVDC Converter

Since a converter is capable of tracking a power reference signal with a time constant of several tens of milliseconds [7], its transient dynamics is not considered here.

Conventionally, in an MT-HVDC system, only one of the converters (indexed by k) regulates the DC voltage, while all the others control the real power exchanged between the AC and the DC sides [8]–[10]. In fact, converter k plays the role of the slack bus that maintains the power balance within the DC grid, and the DC grid can be considered as a real power exchange center between different AC areas. Without loss of generality, we assume an area numbering such that $k = N$.

Formally, with the notations introduced in Section 2.2, $P_1^{dc}, \ldots, P_{N-1}^{dc}$ can be used as control variables to influence the frequencies of the different AC areas, whereas P_N^{dc} is determined by the DC grid load flow to maintain the power balance within the DC grid.

3. Coordinated primary frequency controller

This section first recalls the coordinated control scheme proposed in [4]. Then, the delays potentially involved in the application of this control scheme are discussed and their influence on the system dynamics is modeled.

3.1. Control scheme

The control scheme proposed in [4] is distributed in nature. It is composed of $N - 1$ subcontrollers, one for each HVDC converter except converter N which maintains the voltage of the DC grid. The subcontroller assigned to converter $i \in \{1, \ldots, N-1\}$ modifies the value of P_i^{dc} such that

$$\begin{aligned} \frac{dP_i^{dc}(t)}{dt} =& \alpha \sum_{j=1}^{N} b_{ij}(\Delta f_i(t) - \Delta f_j(t)) \\ &+ \beta \sum_{j=1}^{N} b_{ij} \left(\frac{df_i(t)}{dt} - \frac{df_j(t)}{dt} \right) \end{aligned} \quad (8)$$

where

- $\Delta f_i(t) = f_i(t) - f_{nom,i}$.
- α and β are analogous to integral control gain and proportional control gain, respectively. The influence of their value on the system dynamics will be discussed later in this paper.
- b_{ij} is the coefficient representing the communication graph of the system. The value of b_{ij} equals 1 if subcontroller i receives frequency information on area j, and 0 otherwise.

3.2. Effects of delays

Equation (8) should in principle determine the evolution of P_i^{dc}, which represents the power injected by area i into the HVDC grid. However, a subcontroller based on (8) would lead in a real power system to a variation of P_i^{dc} that may differ significantly from the one defined by this equation.

We believe indeed that the sum of the time necessary to measure the frequencies of the AC areas, transmit these values to subcontroller i, compute a reference value for P_i^{dc}, and apply it to the converter may be significant. This may in turn lead to an effective variation of P_i^{dc} that is delayed with respect to the one predicted by (8).

To give numerical values for these delays, let us note that it takes at least one period, which is around 20ms (resp. 17ms), to measure a frequency close to 50Hz (resp. 60Hz). Concerning the time necessary to encode, transmit, and decode the frequency information from one AC area to another, it is of the order of several hundreds of milliseconds if not one or two seconds. By way of example, the UCTE does not guarantee delays less than 2 seconds for transmitting information from a substation to a remote SCADA system [5]. As to the time necessary for a converter to effectively inject into the HVDC grid a power setting computed by its subcontroller, it can reach up to tens of milliseconds.

In the following, we will study the properties of the control scheme in the presence of such delays. To simplify the study, we will assume that the overall delays are the same regardless of the subcontroller considered and we denote it by τ.

We will also assume that τ affects the power injected by converter i into the HVDC grid in such a way that the dynamics of P_i^{dc} is now given by the following equation:

$$\begin{aligned}\frac{dP_i^{dc}(t)}{dt} =&\alpha \sum_{j=1}^{N} b_{ij}(\Delta f_i(t-\tau) - \Delta f_j(t-\tau)) \\ &+ \beta \sum_{j=1}^{N} b_{ij}\left(\frac{df_i(t-\tau)}{dt} - \frac{df_j(t-\tau)}{dt}\right) .\end{aligned} \tag{9}$$

4. System stability

This section reports a theoretical study on the stability properties of the system in the presence of a delay τ. We prove that for a system subjected to a small step change in the load, there exists a unique equilibrium point, at which the frequency deviations are equal in all AC areas. Then, we study the conditions under which the system converges to that equilibrium point, and we provide a Nyquist stability criterion for the special case where all the AC areas have identical parameters.

The theoretical analysis relies on the following assumptions:

Assumption 1: The losses within the DC grid do not vary with time, i.e.,

$$\sum_{i=1}^{N} \frac{dP_i^{dc}}{dt} = 0 . \tag{10}$$

Assumption 2: The communication graph that represents the frequency information availability at different subcontrollers has the following properties:

- If the subcontroller of one area has access to the information on another area's frequency, then the subcontroller of this second area also has access to the information on the first area's frequency, i.e., if $b_{ij} = 1$, then $b_{ji} = 1, \forall i \neq j, i, j \in \{1, \ldots, N-1\}$. Observe that this property, together with Assumption 1, implies that the time derivative of P_N^{dc} also satisfies (9), where $b_{Ni} = b_{iN}, \forall i \in \{1, \ldots, N\}$.
- The communication graph can not be made of several parts which are not connected to each other, i.e., if $b_{ij} = 0$, then there must exist some intermediate indices $k_1, \ldots, k_m$ such that $b_{ik_1} = b_{k_1k_2} = \ldots = b_{k_mj} = 1$.
- It is constant in time.

Assumption 3: The nonlinear equation (1) can be linearized around $f_i = f_{nom,i}$ as:

$$2\pi J_i \frac{df_i}{dt} = \frac{P_{mi} - P_{li}^o - P_i^{dc}}{2\pi f_{nom,i}} - 2\pi D_{gi}(f_i - f_{nom,i}) . \tag{11}$$

In the following, the HVDC system is modeled by the linear model, where the dynamics of area $i \in \{1, \ldots, N\}$ is defined by (3), (9), and (11).

4.1. Equilibrium point

Proposition 1: Consider that the HVDC system, operating at its nominal equilibrium, is suddenly subjected to a step change in the load of one of its AC areas. Then, under Assumptions 1, 2, and 3, the (linearized) HVDC system has a unique equilibrium point, at which frequency deviations in all AC areas are equal.

Proof: Prior to the step change in the load of one of the AC areas, each AC area is considered in steady state with its frequency regulated at $f_{nom,i}$. We denote the steady-state values by the variables with a bar overhead. After the step change in the load, the variables start to change. We introduce the following incremental variables:

$$\begin{aligned} x_i(t) &= f_i(t) - f_{nom,i} , \\ y_i(t) &= P_{mi}(t) - \bar{P}_{mi} , \\ u_i(t) &= P_i^{dc}(t) - \bar{P}_i^{dc} , \\ v_i(t) &= P_{li}(t) - \bar{P}_{li}^o . \end{aligned}$$

By introducing these variables, (3), (9), and (11) become

$$\frac{dx_i(t)}{dt} = -a_{1i}x_i(t) + a_{2i}y_i(t) - a_{2i}u_i(t) - a_{2i}v_i(t) , \tag{12}$$

$$\frac{dy_i(t)}{dt} = -a_{3i}x_i(t) - a_{4i}y_i(t) , \tag{13}$$

$$\begin{aligned}\frac{du_i(t)}{dt} =&\alpha \sum_{j=1}^{N} b_{ij}(x_i(t-\tau) - x_j(t-\tau)) \\ &+ \beta \sum_{j=1}^{N} b_{ij}\left(\frac{dx_i(t-\tau)}{dt} - \frac{dx_j(t-\tau)}{dt}\right)\end{aligned} \tag{14}$$

where $a_{1i} = D_{gi}/J_i$, $a_{2i} = 1/(4\pi^2 f_{nom,i} J_i)$, $a_{3i} = P_{mi}^{\max}/(T_{smi}\sigma_i f_{nom,i})$, and $a_{4i} = 1/T_{smi}$. Note that a_{1i}, a_{2i}, a_{3i}, and a_{4i} are all positive constants.

Equations (12), (13), and (14) describe the closed-loop dynamics of AC area $i, \forall i \in \{1, \ldots, N\}$, where

the state variables are $x_i(t)$, $y_i(t)$, and $u_i(t)$ and the external input is $v_i(t)$. Initially, all the state variables are equal to zero, since they are defined as the incremental values with respect to the initial nominal equilibrium. At t_0, a step change in load occurs in area m such that:

$$v_i(t) = \begin{cases} \bar{v}_m & \text{for } i = m \text{ and } t > t_0 \ , \\ 0 & \text{otherwise} \ . \end{cases} \quad (15)$$

We now search for equilibrium points of the system following the step change in the load. Let (x_i^e, y_i^e, u_i^e) characterize the state of area i at such an equilibrium point. At this point,

$$\frac{dx_i(t)}{dt} = \frac{dx_i(t-\tau)}{dt} = \frac{dy_i(t)}{dt} = \frac{du_i(t)}{dt} = 0 \ . \quad (16)$$

Thus, (12), (13), and (14) become algebraic equations

$$0 = -a_{1i}x_i^e + a_{2i}y_i^e - a_{2i}u_i^e - a_{2i}v_i(t > t_0) \ , \quad (17)$$

$$0 = -a_{3i}x_i^e - a_{4i}y_i^e \ , \quad (18)$$

$$0 = \alpha \sum_{j=1}^{N} b_{ij}(x_i^e - x_j^e) \ . \quad (19)$$

Equation (19) can be written in matrix form for the entire HVDC system. Define the vector $\mathbf{x}^e = [x_1^e, \ldots, x_N^e]^T$ and let $\mathbf{0}_N$ (resp. $\mathbf{1}_N$) denote the column vector of length N with all components equal to 0 (resp. 1). Then, (19) becomes

$$\mathbf{0}_N = \alpha L \mathbf{x}^e \quad (20)$$

where L is the Laplacian matrix of the communication graph. It is defined by

$$[L]_{ij} = \begin{cases} -b_{ij} & \text{for } i \neq j \ , \\ \sum_j b_{ij} & \text{for } i = j \ . \end{cases} \quad (21)$$

The Laplacian matrix L of a communication graph satisfying Assumption 2 is symmetric positive semidefinite and its only zero eigenvalue corresponds to eigenvector $\mathbf{1}_N$. Therefore equilibrium requires that the frequency deviations in all AC areas are equal. Let x^e be the value of the frequency deviations at the equilibrium point.

From (17) and (18), we obtain

$$y_i^e = -\frac{a_{3i}}{a_{4i}}x^e, \quad (22)$$

$$u_i^e = -\left(\frac{a_{1i}}{a_{2i}} + \frac{a_{3i}}{a_{4i}}\right)x^e - v_i(t > t_0)$$
$$= \begin{cases} -\left(\frac{a_{1i}}{a_{2i}} + \frac{a_{3i}}{a_{4i}}\right)x^e - \bar{v}_m & \text{for } i = m \ , \\ -\left(\frac{a_{1i}}{a_{2i}} + \frac{a_{3i}}{a_{4i}}\right)x^e & \text{otherwise} \ . \end{cases} \quad (23)$$

We see in (23) that if x^e can be uniquely determined, then the equilibrium point exists and is unique. Assumption 1 implies that $\sum_{i=1}^N u_i(t)$ is a constant. The initial conditions yield that $\sum_{i=1}^N u_i(0) = 0$. Thus, $\sum_{i=1}^N u_i^e = 0$. From (23), we see that x^e is uniquely determined as

$$x^e = -\bar{v}_m \cdot \left(\sum_{i=1}^{N} \frac{a_{1i}a_{4i} + a_{2i}a_{3i}}{a_{2i}a_{4i}}\right)^{-1} \ . \quad (24)$$

□

Remark 1: The equilibrium point, which is a static quantity, is of course independent of delay τ. However, delays play a crucial role in the system's convergence towards the equilibrium or not, which we study next.

Remark 2: We assumed above that the step change in the load occurs in only one AC area. However, for the general case where $v_i(t)$ changes in more than one area and eventually settles at $\bar{v}_i$ different from 0, it is straightforward to extend the above results to reach a similar conclusion on the existence of a unique equilibrium point, with x^e given by

$$x^e = -\left(\sum_{i=1}^{N} \bar{v}_i\right) \cdot \left(\sum_{i=1}^{N} \frac{a_{1i}a_{4i} + a_{2i}a_{3i}}{a_{2i}a_{4i}}\right)^{-1} \ . \quad (25)$$

4.2. Stability of the system with identical AC areas

Theoretically proving stability of the control scheme is not an obvious question. We present a result only for the case where all AC areas are assumed identical.

In this subsection we drop AC area index i when referring to the parameters of these areas. We also define the transfer function

$$h(s) = \frac{a_2(s + a_4)}{(s + a_1)(s + a_4) + a_2a_3} \quad (26)$$

where $a_1 = D_g/J$, $a_2 = 1/(4\pi^2 f_{nom} J)$, $a_3 = P_m^{\max}/(T_{sm}\sigma f_{nom})$, and $a_4 = 1/T_{sm}$.

Proposition 2: Consider that all AC areas of the HVDC system have identical parameters, and that Assumptions 1, 2, and 3 are satisfied. Denote by λ_N and λ_2, respectively the largest and smallest non-zero eigenvalues of the Laplacian associated to the communication graph (see (21)). Then the system is stable, and following a step change in the load it asymptotically converges to the unique equilibrium point of Proposition 1, if the net encirclement of any point on the segment $(-1/\lambda_2, -1/\lambda_N)$ by the Nyquist plot of $h(s)(\alpha + \beta s)e^{-\tau s}/s$ is zero.

Proof: Applying the Laplace transform to (12) and (13), we have

$$x_i(s) = \frac{a_2}{s + a_1}y_i(s) - \frac{a_2}{s + a_1}(u_i(s) + v_i(s)) \ , \quad (27)$$

$$y_i(s) = -\frac{a_3}{s+a_4} x_i(s) \ . \tag{28}$$

Eliminating $y_i(s)$ from (27) yields

$$x_i(s) = \frac{-a_2(s+a_4)}{(s+a_1)(s+a_4)+a_2a_3}(u_i(s)+v_i(s)) \ , \tag{29}$$

which, written in matrix form, is

$$\mathbf{x}(s) = -h(s) I_N(\mathbf{u}(s)+\mathbf{v}(s)) \ . \tag{30}$$

By following the same procedure, the dynamics of P_i^{dc} defined by (14) can be expressed in the frequency domain as:

$$u_i(s) = (\frac{\alpha}{s}+\beta)e^{-\tau s}\sum_{j=1}^{N} b_{ij}(x_i(s)-x_j(s)) \ , \tag{31}$$

which can be written in matrix form as:

$$\mathbf{u}(s) = (\frac{\alpha}{s}+\beta)e^{-\tau s} L\mathbf{x}(s) \ . \tag{32}$$

By replacing $\mathbf{u}(s)$ in (30) by (32), we have

$$\mathbf{x}(s) = -s\ h(s)\ (sI_N + h(s)(\alpha+\beta s)e^{-\tau s}L)^{-1}\mathbf{v}(s) \ . \tag{33}$$

Define

$$G_\tau(s) = -s\ h(s)\ (sI_N + h(s)(\alpha+\beta s)e^{-\tau s}L)^{-1} \ . \tag{34}$$

Then, $G_\tau(s)$ is the MIMO transfer function between $\mathbf{v}(s)$, the load change vector, and $\mathbf{x}(s)$, the frequency deviation vector.

The system defined by (33) is asymptotically stable if all the poles of its transfer function $G_\tau(s)$ are on the open left half-plane. Since $h(s)$ is itself a stable transfer function because of the positiveness of a_1, a_2, a_3, and a_4, we only have to investigate the zeros of $Z_\tau(s) = sI_N + h(s)(\alpha+\beta s)e^{-\tau s}L$.

Under Assumption 2, the Laplacian L of the communication graph is positive semidefinite and has a single zero eigenvalue. Thus, $L = VDV^T$ where V is an orthogonal matrix (containing eigenvectors of L) and D is diagonal (containing eigenvalues $0 = \lambda_1 < \lambda_2 \leq \lambda_3 \leq \ldots \leq \lambda_N$). Now $V^T Z_\tau(s) V = sI_N + h(s)(\alpha+\beta s)e^{-\tau s}D$ has the same zeros as $Z_\tau(s)$. A single zero at $s=0$ is obtained with eigenvector of $\lambda_1 = 0$. The latter however cancels with the zero at $s=0$ in the numerator[1] of $G_\tau(s)$. To ensure input-output stability, $Z_\tau(s)$ must be positive definite in the subspace spanned by all other eigenvectors (which we denoted by ω_k), for s in the closed right half-plane. This means that

$$\begin{aligned}
&(sI_N + h(s)(\alpha+\beta s)e^{-\tau s}L)\omega_k \\
=&s\omega_k + \lambda_k h(s)(\alpha+\beta s)e^{-\tau s}\omega_k \\
=&(s+\lambda_k h(s)(\alpha+\beta s)e^{-\tau s})\omega_k \\
=&\mathbf{0}_N
\end{aligned} \tag{35}$$

with $k>1$ may not have solutions in the closed right half-plane. The Nyquist criterion says that this holds if the net encirclement of the point $(-1/\lambda_k, 0)$ by the Nyquist plot of $h(s)(\alpha+\beta s)e^{-\tau s}/s$ is zero. Hence the proposition's requirement. Because the whole system's state is observable from the frequency deviation signals, output (i.e., frequency deviation) stability implies stability of the whole state.

The output corresponding to zero initial conditions and a step input

$$\mathbf{v}(t) = \begin{cases} 0 & \text{for } t<0, \\ \bar{\mathbf{v}} & \text{for } t>0, \end{cases}$$

is then given by

$$\mathbf{x}(s) = G_\tau(s)\mathbf{v}(s) = \tfrac{1}{s}G_\tau(s)\,\bar{\mathbf{v}} \ . \tag{36}$$

As before, we can diagonalize (36) in the basis of eigenvectors of L. From the previous analysis/conditions, components corresponding to λ_k, $k>1$, have negative poles and therefore, according to linear systems theory, exponentially decay to zero. The term $1/s$ in (36) introduced by $v(s)$ is the only term that does not decay away in the output, and in time-domain it corresponds to a step change which represents the shift by x_e of all frequency deviations at equilibrium. □

Remark 3: The above criterion yields that the system defined by (33) is always stable for $\tau = 0$, which is consistent with the theoretical results in [4].

To show this, we denote the argument of $f(s)$ by $\arg(f(s))$ and define

$$\begin{aligned}
J(s) &= \lambda_k h(s)(\alpha+\beta s)/s \\
&= \frac{\lambda_k a_2(s+a_4)(\beta s+\alpha)}{s[(s+a_1)(s+a_4)+a_2a_3]} \ .
\end{aligned} \tag{37}$$

The argument of $J(s)$ can be calculated as:

$$\begin{aligned}
\arg(J(s)) =& \arg(s+a_4) + \arg(\beta s+\alpha) - 90^\circ \\
&- \arg((s+a_1)(s+a_4)+a_2a_3) \ .
\end{aligned}$$

With the definition of all the coefficients in $J(s)$, we have

$$\begin{aligned}
&\arg((s+a_1)(s+a_4)+a_2a_3) \\
<&\arg((s+a_1)(s+a_4))
\end{aligned}$$

1. This does not correspond to the pole cancellation control. As a matter of fact, the "s" factors in denominator and numerator also cancel for the open-loop system, which is stable. The factors "s" come from rewriting our dynamics, so the pole and zero at $s=0$ always cancel exactly.

$$= \arg(s+a_1) + \arg(s+a_4)\ ,$$

from which

$$\begin{aligned}\arg(J(s)) &> \arg(\beta s+\alpha) - 90^\circ - \arg(s+a_1)\\ &> -180^\circ\ .\end{aligned}$$

On the other hand, it is straightforward to see that $\arg(J(s)) < 180^\circ$. Thus, the Nyquist plot of $J(s)$ can not intersect with the negative real axis as s grows from $j0$ to $j\infty$, where $j = \sqrt{-1}$. Therefore, the points on the segment $(-1/\lambda_2, -1/\lambda_N)$ are never encircled, which, according to Proposition 2, implies that the system is always stable for $\tau = 0$.

5. Simulations

To analyze the effects of the delays on the performances of our control scheme, simulations are conducted on an HVDC system with five non-identical non-synchronous areas, which is described in the first part of this section.

5.1. Benchmark system

The benchmark system consists of a multi-terminal HVDC grid connecting five non-synchronous areas. The converter of area 5 is chosen to regulate the DC voltage, whose setting is 100kV. The topology of the DC network is represented in Fig. 2. The communication graph coincides with the network topology, i.e., each edge in the figure also represents a bi-directional communication channel between the two areas it connects. The resistance of the DC links are: $R_{12} = 139\Omega$, $R_{15} = 417\Omega$, $R_{23} = 278\Omega$, $R_{25} = 695\Omega$, $R_{34} = 278\Omega$, and $R_{45} = 278\Omega$. In our simulations, we consider that individual AC areas significantly differ from each other, see the parameters in Table 1.

To observe the system's response to a step change in the load, we assume that all the areas operate originally in steady state at their nominal frequency. Then at time $t = 2$s, a 5% increase of the value of P^o_{l2} (see (4)) is modeled.

The continuous-time differential equations (3), (9), and (11) are integrated in this paper using an Euler method with a time-discretization step of 1ms.

5.2. Effects of the delays

Simulations reported in [4] show that for $\tau = 0$s, the control scheme (8) drives the frequency deviations of all the areas to the same value. Additionally, when the frequencies are stabilized, the frequency in area 2 is equal to a value which is closer to $f_{nom,2}$ than when the DC converters are operated with constant power injection.

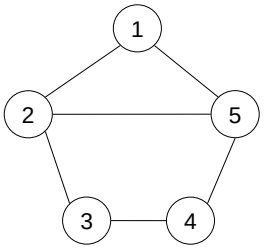

Figure 2. DC grid topology. The circle numbered i represents the point in the DC grid to which converter i is connected. An edge between two circles represents a DC line.

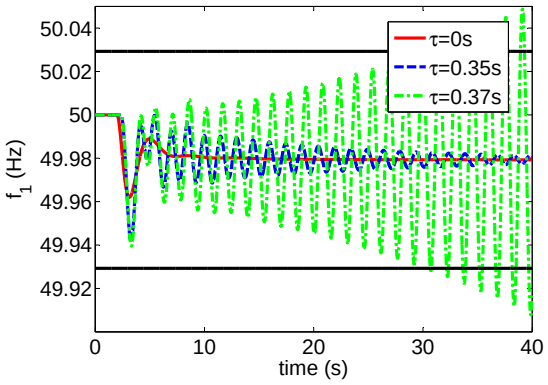

Figure 3. Frequency of AC area 1 for $\tau = 0$s, $\tau = 0.35$s, and $\tau = 0.37$s when $\alpha = \beta = 4.44 \times 10^6$. The two horizontal lines draw the band of the convergence criterion, which is $\pm$50mHz around Δf^e.

In contrast, with delays, simulations show that the frequency deviations may fail to converge to each other. In particular, for given values of α and β, there generally exists a maximum acceptable delay beyond which the AC areas' frequencies exhibit oscillations of increasingly large magnitude. For example, when the controller gains are empirically chosen to be 4.44×10^6, f_1 still converges despite oscillations when $\tau = 0.35$s and fails to converge when $\tau = 0.37$s, as shown in Fig. 3. For comparison, the evolution of f_1 when $\tau = 0$s is also shown in the same figure.

To determine whether the frequency deviations of all the AC areas converge to each other, we define the following criterion, similar to the error band used in

Table 1. Parameter values for the AC areas.

Parameter	Area					Unit
	1	2	3	4	5	
f_{nom}	50	50	50	50	50	Hz
P_m^o	50	80	50	30	80	MW
$P_m^{\max}$	100	160	100	60	160	MW
J	2026	6485	6078	2432	2863	kg/s^2
D_g	30.5	92.0	88.0	34.5	59.7	kW $\cdot$ s/rad
σ	0.05	0.10	0.15	0.10	0.075	
T_{sm}	1.5	2.0	2.5	2	1.8	s
P_l^o	100	60	40	50	30	MW
D_l	0.01	0.01	0.01	0.01	0.01	s

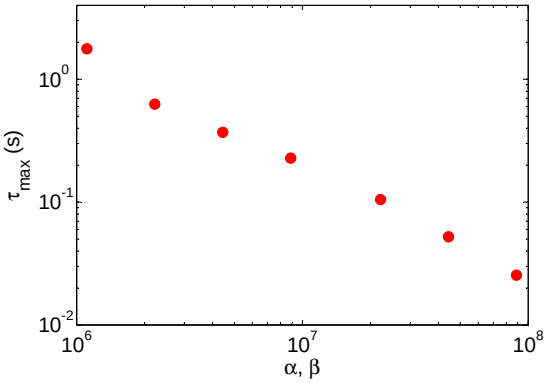

Figure 4. Values of $\tau_{\max}$ for several values of $\alpha = \beta$.

the definition of settling time in control theory [11]. Let us denote by Δf^e the common value to which the frequency deviations of all AC areas converge when $\tau = 0$s. We classify the system as convergent as long as after $t > 22$s, i.e., 20 seconds after the step change in the load, all the AC areas' frequency deviations remain within $\pm$ 50mHz around Δf^e, i.e.,

$$|\Delta f_i(t) - \Delta f^e| \leq 50\text{mHz}, \forall i \text{ and } \forall t > 20\text{s} \ . \quad (38)$$

We define $\tau_{\max}$ as the largest value of the delay for which (38) is satisfied and we search for a relation that may exist between $\tau_{\max}$ and the controller gains. To ease the analysis, we impose that $\alpha = \beta$. We compute $\tau_{\max}$ for different $\alpha = \beta \in [1 \times 10^6, 1 \times 10^8]$ by a binary search in $\tau \in [0, 4]$s. The points in Fig. 4 represent values of $\tau_{\max}$ corresponding to different $\alpha = \beta$. We can see that by decreasing the values of the controller gains, the harmful oscillations introduced by delays can be curbed. For example, if τ is around two seconds for our system, then we have to decrease the controller gains to a value around 1×10^6 to avoid convergence problems. However, as pointed out in [4], with lower values of the controller gains, more time is needed for the frequency deviations to converge to similar values.

This phenomenon is illustrated here in the context of a power system with delays by the two sets of curves of Fig. 5 that represent the evolution of the frequencies in the five areas of the system for $\alpha = \beta = 1 \times 10^6$ and for $\alpha = \beta = 1 \times 10^5$. Note that we have also represented in these figures the evolution of f_2 when no control scheme is implemented (i.e., when the power injections into the DC network remain constant).

6. Conclusions

This paper focuses on a previously proposed control scheme to share primary frequency control reserves among non-synchronous systems connected by a multi-terminal HVDC grid. We have studied here the effects of delays on the effectiveness of this control scheme. The study is both analytical and empirical. In particular, we have derived, under some restrictive assumptions on the power system, a stability criterion that may be used to compute the maximum acceptable value for the delay so as to ensure that the control scheme does not lead to stability problems. We have also reported simulation results showing that for delays above a threshold value, the control scheme may cause undamped frequency oscillations. Additionally, as shown by these simulations, these undamped frequency oscillations are more likely to appear when using high values of the controller gains.

As future work, we suggest to extend the theoretical study of the control scheme, notably to the case of non-identical AC areas. We also believe that it would be interesting to test this control scheme on more sophisticated power system benchmarks such as those

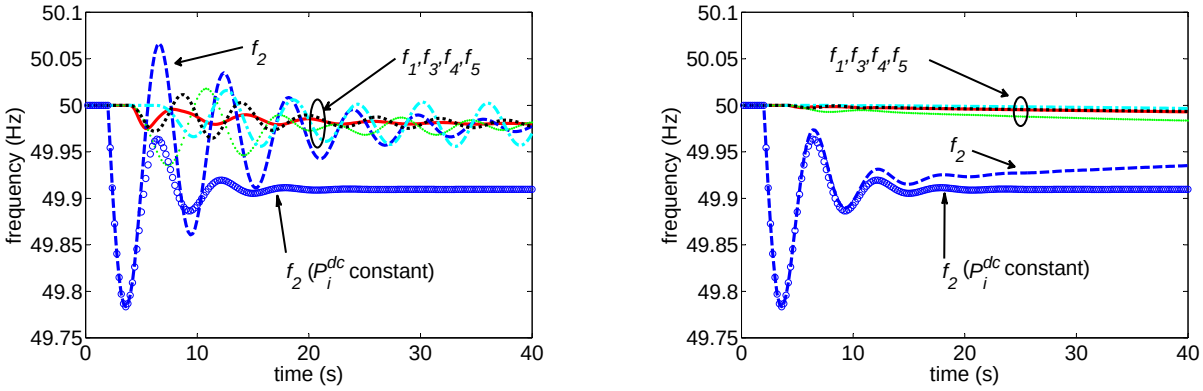

Figure 5. Frequencies of the five AC areas when $\tau = 2$s for $\alpha = \beta = 1 \times 10^6$ (on the left) and for $\alpha = \beta = 1 \times 10^5$ (on the right). Both figures also include the evolution of f_2 when the power injections into the DC network remain constant.

that would not neglect for example voltage regulation in the AC areas.

Acknowledgment

Alain Sarlette is a FRS-FNRS postdoctoral research fellow and Damien Ernst is a FRS-FNRS research fellow. They thank the FRS-FNRS for its financial support. They also thank the financial support of the Belgian Network DYSCO, an Interuniversity Attraction Poles Programme initiated by the Belgian State, Science Policy Office. Alain Sarlette was an invited researcher at the Ecole des Mines de Paris when carrying out this research. The scientific responsibility rests with its authors.

References

[1] P. Kundur, J. Paserba, V. Ajjarapu, G. Andersson, A. Bose, C. Canizares, N. Hatziargyriou, D. Hill, A. Stankovic, C. Taylor, T. Van Cutsem, and V. Vittal, "Definition and classification of power system stability," *IEEE Transactions on Power Systems*, vol. 19, pp. 1387–1401, August 2004.

[2] Y. G. Rebours, D. S. Kirschen, M. Trotignon, and S. Rossignol, "A survey of frequency and voltage control ancillary services – part I: Technical features," *IEEE Transactions on Power Systems*, vol. 22, pp. 350–357, February 2007.

[3] R. Grünbaum, B. Halvarsson, and A. Wilk-Wilczynski, "FACTS and HVDC Light for power system interconnections," in *Power Delivery Conference*, (Madrid, Spain), September 1999.

[4] J. Dai, Y. Phulpin, A. Sarlette, and D. Ernst, "Coordinated primary frequency control among non-synchronous systems connected by a multi-terminal HVDC grid," Submitted.

[5] "UCTE operation handbook," July 2004.

[6] P. Kundur, *Power System Stability and Control*. McGraw-Hill, 1994.

[7] J. Arrillaga, *High Voltage Direct Current Transmission*. No. 29 in Power and Energy Series, The Institution of Electrical Engineers, 1998.

[8] V. F. Lescale, A. Kumar, L.-E. Juhlin, H. Bjorklund, and K. Nyberg, "Challenges with multi-terminal UHVDC transmissions," in *Joint International Conference on Power System Technology and IEEE Power India Conference, 2008. POWERCON 2008*, pp. 1–7, August 2008.

[9] H. Jiang and A. Ekström, "Multiterminal HVDC system in urban areas of large cities," *IEEE Transactions on Power Delivery*, vol. 13, pp. 1278–1284, October 1998.

[10] L. Xu, B. Williams, and L. Yao, "Multi-terminal DC transmission systems for connecting large offshore wind farms," in *2008 IEEE Power and Energy Society General Meeting - Conversion and Delivery of Electrical Energy in the 21st Century*, (Pittsburgh, PA), pp. 1–7, July 2008.

[11] K. Ogata, *Modern Control Engineering*. Prentice Hall, 5 ed., September 2009.